Vol 18 No 3, March 2009
1674-1056/2009/18(03)/1177-04
Chinese Physics B
© 2009 Chin. Phys. Soc.
and IOP Publishing Ltd

Numerical simulation of super-short pulsed discharge in helium with particle-in-cell Monte Carlo collisions technique*

Shi Feng(石 锋), Zhang Li-Li(张莉丽), and Wang De-Zhen(王德真)†

School of Physics and Optoelectronic Technology, Dalian University of Technology, Dalian 116024, China

(Received 14 May 2008; revised manuscript received 20 July 2008)

This paper reports that a simulation of glow discharge in pure helium gas at the pressure of 1.333×10^3 Pa under a high-voltage nanosecond pulse is performed by using a one-dimensional particle-in-cell Monte Carlo collisions (PIC–MCC) model. Numerical modelling results show that the cathode sheath is much thicker than that of anode during the pulse discharge, and that there exists the phenomenon of field reversal at relative high pressures near the end of the pulse, which results from the cumulative positive charges due to their finite mobility during the cathode sheath expansion. Moreover, electron energy distribution function (EEDF) and ion energy distribution function (IEDF) have been also observed. In the early stage of the pulse, a large amount of electrons can be accelerated above the ionization threshold energy. However, in the second half of the pulse, as the field in bulk plasma decreases and thereafter the reverse field forms due to the excessive charges in cathode sheath, although the plasma density grows, the high energy part of EEDF decreases. It concludes that the large volume non-equilibrium plasmas can be obtained with high-voltage nanosecond pulse discharges.

Keywords: high-voltage nanosecond pulse, PIC–MCC model, EEDF, IEDF
PACC: 5265, 5280, 5220

1. Introduction

How to produce and stabilize large-volume low temperature plasma at a relatively higher pressure, from a few Torrs to hundreds of Torrs (1 Torr=133.332 Pa), has been paid more and more attentions along with the development of technology and engineering due to their practical and potential applications.[1−4] High-voltage nanosecond pulse methods,[5] one of the most promising ways to obtain such plasmas, have been used and studied in various processes in industry and research,[6,7] including producing free radicals in plasma chemistry processes,[8] material processing,[9,10] environmental and biotechnological applications.[11] Hence, the study of pulsed discharges producing large-volume non-equilibrium plasma becomes a valuable subject.

Several approaches have been used to give insights to these non-equilibrium plasmas at high pressures. With fluid models,[12−14] plasma density, temperature and heating power are obtained. In these models, the electrons' energy distribution is assumed to be Maxwellian distribution with a given temperature. However, when non-equilibrium plasma at a higher pressure, from several Torrs to one atmospheric pressure,[15,16] is sustained by an external power, the electron energy distribution function (EEDF), which reveals electrons' acceleration and energy gaining efficiency in the gas discharge and determines the chief discharge characteristics of these non-equilibrium plasma,[1,17] is obviously non-Maxwellian distribution.[18,19] That is, electrons in the high energy tail may significantly influence or even determinate the plasma discharge properties. Although kinetic models by solving Boltzmann equations could present us some useful insights of EEDF by using 'forward–backward' approximation,[3] the accurate results without such assumptions have not been obtained in the same conditions. Therefore, in this paper, we have adopted the particle-in-cell Monte Carlo collisions (PIC–MCC) model to simulate the non-equilibrium pulse discharge plasma with the pressure of 10 Torr, and obtained some key characteristics of spatial–temporal plasma during a short high-voltage pulse discharge.

*Project supported by the National Natural Science Foundation of China (Grant No 10775027).
†E-mail: wangdez@dlut.edu.cn

2. Model descriptions and initial conditions

A pure helium gas model is adopted in this paper. The electron and ion kinetic equations are included in the PIC–MCC model.[20−23] To be brief, initially, each electron and each ion in the simulation are assigned individually positions (one-dimensional), velocities (three-dimensional), and their own weights. The particle motions under the applied power, as well as the electric field, are then traced in each time interval until the desired time is reached in the simulation.

Each step can be outlined as follows. In the first step, all the charged particles' positions are linearly interpolated to the nearest mesh point in order to obtain ion and electron spatial densities at a new time (just at the beginning of a time interval) so that one can calculate the value of the electrostatic potential and field at each grid point in space by solving the Poisson's equation. In the second step, the one-dimensional position, $\boldsymbol{x}$, and three-dimensional velocities, $\mathbf{v}$, of every traced particle, are renewed at the end of each time section in the simulation based on the kinetic equations, $\boldsymbol{F} = q\boldsymbol{E}(\boldsymbol{x}, t)$, $\boldsymbol{v}(t) = \mathrm{d}\boldsymbol{x}(t)/\mathrm{d}t$, and $\boldsymbol{F}(\boldsymbol{x}, t) = M \cdot \mathrm{d}\boldsymbol{v}(t)/\mathrm{d}t$. Besides, the boundary condition of the electric potential is known as the applied voltage, so we can solve the Poisson's equation for the potential at the mesh point. Note that the electric field $\boldsymbol{E}(\boldsymbol{x}, t)$ is also obtained just at the mesh point constructed by PIC model through the solutions of potential difference equation. In the third step, the particles that moved beyond the boundaries during the time interval are eliminated from the PIC–MCC simulation. The effect of secondary electron emission at the electrodes is not included in our work because few ions could reach the absorbing electrodes in the time scale of our interest here. In the fourth step, to determine the collision events during the flight time of each particle, a MCC model is employed. The MCCs coupled to PIC can only change the velocities of particles, and do not influence their coordinates in space and their weights. The collisions we have taken into account include electron-neutral and ion-neutral scattering events. The excitation cross sections for electron-neutral collisions in helium can be obtained by using the data from Ref.[24]. Other cross sections, including the electron-neutral elastic collision cross section, the electron-neutral ionization cross section and the ion-neutral charge exchange cross section, can be found in Ref.[25]. In the fifth step, the simulation returns to step one, and the iterative loop continues until the desired time is reached.

The electrodes, which have a distance of 3cm plotted uniformly 10^3 grids between them, are powered by a trapezoidal shape voltage pulse on the anode while the cathode is grounded. Each time step in the simulations is set as 2×10^{-12} s, and each grid holds 100 cells initially. The shape of the pulse can be described as follows: rise in 0.5 ns, up to 9.6 kV, and drop in 0.5 ns, with plateau in 0.25 ns, respectively. The uniform initial electron and ion densities are both $10^{12}/\mathrm{cm}^3$. Such a high and uniform initial plasma density is a natural result of the last pulse in a repetitive nanosecond discharge. Note that, due to the rather small duty cycle, the former pluses do not influence the latter ones noticeably. Therefore, it is also reasonable to assume that the initial velocities of electrons and ions satisfy Maxwellian distributions with the electron temperature of 2 eV and ion temperature of 300 K (room temperature).[3] The validity of our simulations is verified by the comparison with the Ref.[25].

3. Results and discussions

The spatial–temporal evolutions of electron and ion densities in helium at the time of 0.75 ns, 1.15 ns and 3ns are shown in Fig.1, from which we can distinctly see the evolution of both sheaths and plasma volume during the discharge.

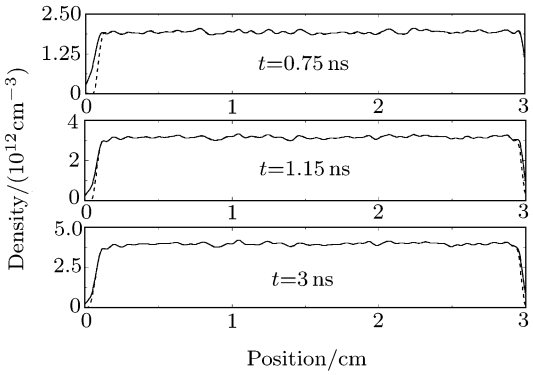


Fig.1. The profiles of electron density(dash line), n_e, ion density(solid line), n_i, at the moment of 0.75 ns, 1.15 ns and 3 ns, respectively, in helium.

The maximum plasma density in the discharge can be up to about $3.5 \times 10^{12}/\mathrm{cm}^3$ in the simulation due to avalanche ionization. The cathode sheath is much thicker than the anode sheath during the pulse, although we have applied a positive high-voltage pulse

on the anode. This is because in our interesting time scale here, about a few nanoseconds, the ions almost keep stationary in comparison with the fast electrons. Near the cathode, the electrons are pulled out of that region while leaving the ions behind. However, although electrons near the anode are rapidly pulled onto the anode, the electrons from the plasma volume could quickly move into the anode region, so we can hardly recognize the anode sheath during the pulse. Thus, as the evolution of the discharge, the cathode sheath is more and more thicker than that of anode. This cumulative charged particles' effect leads to a notable phenomenon of 'field reversal', which was obtained and explained for the first time in Ref.[26], shown in Fig.2. That is, a local motion-opposing space field to electrons forms.

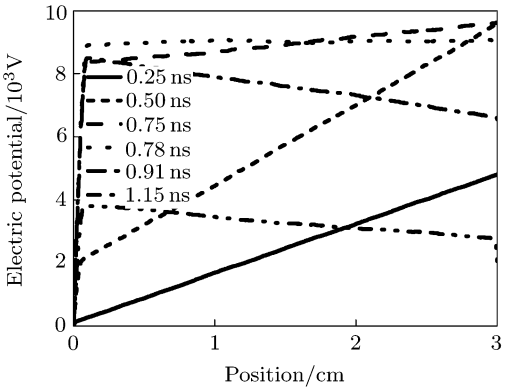


Fig.2. Electrostatic potential profiles at different times.

From Fig.2 we can clearly see the evolution of the field along the discharge gap. With the growth of avalanche ionization, the cathode sheath develops while the strong electric field in cathode sheath remains almost the same. The field in that region is strong enough to speed up the electrons resulting in further ionizations in bulk plasma while leaving behind the ions near the cathode because of their finite mobility. This cumulative charge effect eventually makes the field in the bulk plasma reverse near the end of the pulse. From Fig.2, we can also see that, the field reversal effect appears at about 0.78 ns. It is noted that, the moment of field reversal effect in helium predicted by PIC–MCC model (0.78 ns) is earlier than the hydrodynamic model in air (0.91 ns).[5] This result reveals that the fluid models do not exactly address the high energy tail of EEDF, while the PIC–MCC model could present us the detailed statistical information of this region of EEDF in the discharges. This leads to the fact that the avalanche ionization develops differently between two models, and we believe that the PIC–MCC model could reflect the realistic cases more accurately in the discharges.

The spatial–temporal evolution profiles of EEDF and ion energy distribution function (IEDF) are also given in Figs.3 and 4, respectively. From these figures, we can see that a large number of electrons can be rapidly speeded up above the threshold energy of ionization and cause avalanche ionization in the early stage of the discharge.

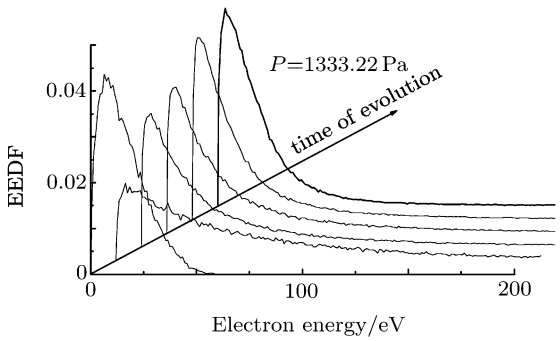


Fig.3. Evolution of the space averaged normalized electron energy distribution function at different times: 0.25 ns, 0.50 ns, 0.75 ns, 0.78 ns, 0.81 ns, 1.15 ns.

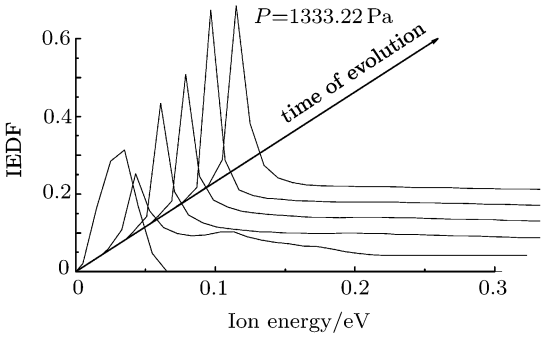


Fig.4. Evolution of the space averaged normalized ion energy distribution function at different times: 0.25 ns, 0.50 ns, 0.75 ns, 0.78 ns, 0.81 ns, 1.15 ns.

As we can see from Fig.2, at the beginning of the pulse, the potential is quite linear along the discharge gap and the sheaths are not very clear. As the discharge evolves, the potential in both plasma volume and cathode sheath increases dramatically but also remains linear. Note that, the field in the bulk plasma reaches the maximum at about 0.50 ns. That is, the electrons are significantly speeded up by the applied power in plasma volume at 0.50 ns. So the high energy electrons take a larger amount of the EEDF at 0.50 ns than previous times in the discharge. But this is not the case with further development of the discharge.

Although the field in the cathode sheath keeps constant, the field in the bulk plasma decreases and even to reverse, so the electrons along the discharge gap are not as much as they can be accelerated at 0.50 ns. Therefore, after 0.50 ns, the proportion of the high energy electrons in EEDF decreases, as shown in Fig.3. Note that, the reverse field in bulk plasma remains almost the same, and this field can also accelerate the electrons in plasma volume and sustain the afterglow discharge. Therefore, from Fig.1, we can see that the density of plasma between the electrodes also grows even though the pulse is over. From Fig.4, we can conclude that it is still the non-equilibrium cold plasma with the development of the discharge, and there are few ions can be accelerated, so it is also reasonable to assume that the ions are stationary and form a positive background in super short-pulse discharges.

4. Conclusions

In this paper, we have analysed some key characteristics of discharge in a high-voltage nanosecond pulse in helium at 1333.22 Pa by using the 1d3v PIC–MCC model. The effect of field reversal is particularly observed, since it is considered that the cumulative space charges in both sheaths result in this. In addition, taking the full advantage of the PIC–MCC model, we obtained the evolution of EEDF and IEDF, which could not be obtained by fluid models. It has been shown that the electrons can be speeded up rapidly while the ions remain cooling during the pulse discharge, and that the electrons in the high energy tails can significantly influence the discharge process. It is also quite interesting to note that when the reverse field effect occurs near the end of the pulse, although the electrons in the cathode sheath are accelerated toward the anode, they are forced by the opposite direction field in the bulk plasma. Thus, the high energy part of electrons in EEDF decreases with the increasing plasma density after the establishment of the reverse field. The comparison between fluid model results and PIC–MCC model simulations indicates that the electrons in the high energy tail of EEDF play essential role in gas discharges, and it is concluded that these electrons must be treated precisely at higher pressure of discharges.

References

[1] Kunhardt E E 2000 *IEEE Trans. Pla. Sci.* **28** 189
[2] Hallac A, Georghiou G E and Metaxas A C 2003 *J. Phys.* D: *Appl. Phys.* **36** 2498
[3] Macheret S O, Shneider M N and Miles R B 2002 *IEEE Trans. Pla. Sci.* **30** 1301
[4] Macheret S O, Shneider M N and Murray R C 2006 *Phys. Plas.* **13** 023502
[5] Aleksandrov N L, Kindysheva S V, Kirpichnikov A A, Kosarev I N, Starikovskaia S M and Starikovskii A Yu 2007 *J. Phys.* D: *Appl. Phys.* **40** 4493
[6] Kudlacek P, Vlcek J, Burcalova K and Luka J 2008 *Plas. Sour. Sci. Technol.* **17** 025010
[7] He Z H, Yu F S, Hu F, Yuan Y, Guo L N and Li J 2007 *Plas. Sci. Tech.* **9** 706
[8] Zhang R B, Wu Y and Li G F 2005 *Plas. Sources Sci. Technol.* **14** 308
[9] Göktas H, Oke G and Udrea M 2003 *Turk. J. Phys.* **27** 77
[10] Ehiasarian A P, Hovsepian P Eh, Hultman L and Helmersson U 2004 *Thin Solid Films* **457** 270
[11] Sato M 2008 *Plas. Sources Sci. Technol.* **17** 024021
[12] Shang W L, Wang D Z and Kong M G 2007 *Chin. Phys.* **16** 485
[13] Shang W L and Wang D Z 2007 *Chin. Phys. Lett.* **24** 1992
[14] Chen G Y and Raja L L 2004 *J. Appl. Phys.* **96** 6073
[15] Yang W D, Wang P N, Liu Z P, Mi L and Li F M 2002 *Chin. Phys.* **11** 260
[16] Li X C, Dong L F and Wang L 2005 *Chin. Phys.* **14** 1418
[17] Boeuf J P and Kunhardt E E 1986 *J. Appl. Phys.* **60** 915
[18] Surendra M and Graves D B 1991 *IEEE Trans. Pla. Sci.* **19** 144
[19] Surendra M, Graves D B and Jellum G M 1990 *Phys. Rev.* A **15** 1112
[20] Birdsall C K 1991 *IEEE Trans. Pla. Sci.* **19** 65
[21] Lee S H, Iza F and Lee J K 2006 *Phys. Plas.* **13** 057102
[22] Vahedi V and Surendra M 1995 *Comput. Phys. Commun.* **87** 179
[23] Birdsall C K and Langdon A B 1985 *Plasma Physics via Computer Simulation* (New York: McGraw-Hill) p8
[24] Boeuf J P and Marode E 1982 *J. Phys.* D: *Appl. Phys.* **15** 2169
[25] Nitschke T E and Graves D B 1994 *J. Appl. Phys.* **76** 5646
[26] Raizer Yu P and Shneider M N 1989 *High Temp.* **27** 329